Article

WUE and CO2 Estimations by Eddy Covariance and Remote Sensing in Different Tropical Biomes

Gabriel B. Costa [1,2,3,*], Cláudio M. Santos e Silva [2,4], Keila R. Mendes [4], José G. M. dos Santos [5], Theomar T. A. T. Neves [6], Alex S. Silva [6], Thiago R. Rodrigues [7], Jonh B. Silva [8], Higo J. Dalmagro [9], Pedro R. Mutti [2,4], Hildo G. G. C. Nunes [10], Lucas V. Peres [6], Raoni A. S. Santana [6], Losany B. Viana [6], Gabriele V. Almeida [6], Bergson G. Bezerra [2,4], Thiago V. Marques [11], Rosaria R. Ferreira [4], Cristiano P. Oliveira [2,4], Weber A. Gonçalves [2,4], Suany Campos [2] and Maria U. G. Andrade [2]

[1] Biosciences Post-Graduate Program (PPG-BIO), Federal University of Western Pará (UFOPA), Santarém 68035-110, Brazil
[2] Climate Sciences Post-Graduate Program (PPGCC), Federal University of Rio Grande do Norte (UFRN), Avenue Senador Salgado Filho, 3000, Lagoa Nova, Natal 59078-970, Brazil; claudio.silva@ufrn.br (C.M.S.e.S.); pedro.mutti@ufrn.br (P.R.M.); bergson.bezerra@ufrn.br (B.G.B.); cristiano.prestrelo@ufrn.br (C.P.O.); weber.goncalves@ufrn.br (W.A.G.); suany.csilva@escola.seduc.pa.gov.br (S.C.); uilhiana.andrade.016@ufrn.edu.br (M.U.G.A.)
[3] Anthropic Studies in the Amazon Post-Graduate Program (PPGEAA), Federal University of Pará, Castanhal 68740-222, Brazil
[4] Departamento de Ciências Atmosféricas e Climáticas (DCAC), Universidade Federal do Rio Grande do Norte, Natal 59078-970, Brazil; keila.mendes@icmbio.gov.br (K.R.M.); rosaria@ufrn.edu.br (R.R.F.)
[5] Wildfire Monitoring Program, National Institute for Space Research, São José dos Campos 12227-010, Brazil; guilherme.martins@inpe.br
[6] Institute of Engineering and Geosciences, Federal University of Western Pará (UFOPA), Santarém 68035-110, Brazil; theomar.neves@ufopa.edu.br (T.T.A.T.N.); alex.ss@ufopa.edu.br (A.S.S.); lucas.peres@ufopa.edu.br (L.V.P.); raoni.santana@ufopa.edu.br (R.A.S.S.); losany.viana@discente.ufopa.edu.br (L.B.V.); gabriele.almeida@discente.ufopa.edu.br (G.V.A.)
[7] Laboratório de Ciências Atmosféricas, Universidade Federal de Mato Grosso Do Sul, Campo Grande 79070-900, Brazil; thiago.r.rodrigues@ufms.br
[8] Programa de Pós-Graduação em Física Ambiental, Instituto de Física, Universidade Federal de Mato Grosso, Cuiabá 78060-900, Brazil; jonh_billy@fisica.ufmt.br
[9] Programa de Pós-Graduação em Ciências Ambientais, Universidade de Cuiabá (UNIC), Cuiabá 78060-900, Brazil; higo.dalmagro@educadores.net.br
[10] Socio-Environmental and Water Resources, Federal Rural University of the Amazon, Belém 66077-830, Brazil; garibalde13@gmail.com
[11] Federal Institute of Education, Science and Technology of Rio Grande do Norte, Natal 59628-330, Brazil; thiago.valentim@ifrn.edu.br
[*] Correspondence: gabriel.costa@ufopa.edu.br

Abstract: The analysis of gross primary production (GPP) is crucial to better understand CO_2 exchanges between terrestrial ecosystems and the atmosphere, while the quantification of water-use efficiency (WUE) allows for the estimation of the compensation between carbon gained and water lost by the ecosystem. Understanding these dynamics is essential to better comprehend the responses of environments to ongoing climatic changes. The objective of the present study was to analyze, through AMERIFLUX and LBA network measurements, the variability of GPP and WUE in four distinct tropical biomes in Brazil: Pantanal, Amazonia, Caatinga and Cerrado (savanna). Furthermore, data measured by eddy covariance systems were used to assess remotely sensed GPP products (MOD17). We found a distinct seasonality of meteorological variables and energy fluxes with different latent heat controls regarding available energy in each site. Remotely sensed GPP was satisfactorily related with observed data, despite weak correlations in interannual estimates and consistent overestimations and underestimations during certain months. WUE was strongly dependent on water availability, with values of 0.95 gC kg^{-1} H$_2$O (5.79 gC kg^{-1} H$_2$O) in the wetter (drier) sites. These values reveal new thresholds that had not been previously reported in the literature. Our findings have crucial implications for ecosystem management and the design of climate policies regarding the conservation

of tropical biomes, since WUE is expected to change in the ongoing climate change scenario that indicates an increase in frequency and severity of dry periods.

1. Introduction

Discussions on climate change have become increasingly more relevant in the general scientific community, particularly since the creation of the Intergovernmental Panel on Climate Change (IPCC), which is composed of a diverse group of worldwide researchers, focusing on climate change studies and its impacts on society. Since the industrial revolution, the concentration of carbon dioxide (CO_2) in the atmosphere has increased with the use of fossil fuels, deforestation, the use of nitrogen in agriculture and livestock farming, which are reported to be the main uses responsible for the anthropic greenhouse effect. Studies have already shown the relevance of biosphere–atmosphere interactions in Brazilian biomes regarding planetary climate regulation due, for example, to water, energy, and carbon exchanges with the atmosphere [1–6]. However, there are still uncertainties regarding these processes due to the remarkable diversity of physiognomies, landscapes and other biophysical aspects that might play a role in differentiating atmospheric patterns from one place to another within each biome.

To reduce these uncertainties, in situ measurements are needed to better understand the particularities of each environment. Furthermore, these observed data can also be used to assess soil–vegetation–atmosphere models [7–10] and to analyze satellite-derived estimates of water and/or CO_2 balance components [11–16]. Both these models and remote sensing data are extremely important in providing reliable information on CO_2 exchanges over tropical forests where flux tower coverage is scarce or non-existent, such as in many parts of Brazil.

Additionally, certain forest physiognomies are not endemic to Brazil, but occur in several other regions of the globe, and therefore, their particularities regarding biophysical patterns need to be understood in detail. Wetlands in tropical rainforests such as the Amazon are environments where organic production rates are high and anoxic conditions are frequent, and therefore, they represent crucial zones for the global balance of greenhouse gases in the atmosphere. Cerrado ecosystems (savannas), however, are located at the tropics and subtropics and are characterized by marked wet and dry seasons. They cover approximately 60%, 50% and 45% of the total area of Africa, Australia and South America, respectively [17]. These ecosystems play an important role in the cycle of several greenhouse gasses, as reported by the studies [18–20] among others, and on energy fluxes (latent and sensible heat) in the context of climate change, since they cover approximately 20% (2.7 billion ha) of the global surface [17].

Carbon dynamics and biophysical evapotranspiration controls over tropical Brazilian ecosystems and in other regions of the world have also been studied because of the need to better understand the effects of land use change on regional and global biogeochemical cycles [13,15,21]. Evidently, it also allows us to estimate the contribution of tropical biomes to the regional and global climate controls, also comprising the relationship between precipitation, evapotranspiration, plant productivity and greenhouse gas exchanges within the atmosphere [22]. These changes motivated the development of various research fields within climate sciences focusing on the debate over greenhouse gases cycles and anthropic influence over these cycles. CO_2 concentration in the atmosphere surpassed 405 ppm [23] and continues increasing each decade, as well as that of other greenhouse gases. Therefore, it is necessary to develop methods and techniques to quantify these emissions and the fluxes of these gases, improving the understanding on how different environments function and respond to land-use changes.

The eddy covariance method (EC) directly and non-intrusively estimates the vertical transport of CO_2 and other greenhouse gases. Information measured through EC allows for the better comprehension of biogeochemical cycles, energy fluxes and other atmospheric controls. It also provides clues to other pivotal questions regarding ecosystem (in this study, tropical ecosystems) controls over climate. However, due to the lack of an extensive EC measurement network throughout Brazil, other data sources are required, such as satellite-derived data. Our hypothesis is that both gross primary production (GPP) and water-use efficiency (WUE) data respond differently to varied water availability conditions on the main tropical ecosystems in Brazil. Thus, our objective is to analyze the dynamics of GPP and WUE in the Amazon, Cerrado (savanna), Pantanal and Caatinga biomes through data collected through EC systems and to assess the performance of data derived from the Moderate Resolution Imaging Spectroradiometer (MODIS) sensor for the quantification of CO_2 balance components over these environments.

2. Materials and Methods

2.1. Data Policy and Use License

The Ameriflux platform compiles data monitored in three Brazilian biomes: BR-Sa1 (Amazon), BR-CST (Caatinga) and BR-Npw (Pantanal). Data from the Cerrado site (BR-BI, Bananal Island—Javaés) are available at https://daac.ornl.gov (accessed on 25 April 2022). Data provided by the ORNL DAAC can be accessed for free, without restrictions and in accordance with NASA's Earth Science Program. Ameriflux data are shared under CC-BY-4.0 data usage license (Creative Commons by Attribution 4.0 International). This license states that the use of data is free to share (copy and redistribute the material in any medium or format) and/or adapt (remix, transform, and build upon the material). The scientific literature references describing each of the data sites are: BR-Sa1 [24], BR-CST [25] and BR-Npw [26].

2.2. Description of Study Area

2.2.1. Cerrado Site

Measurements were conducted on an experimental site located on an inundation plain at Cantão State Park, 260 km west of the city of Palmas (Tocantins state, Figure 1) as a part of the Large-Scale Biosphere-Atmosphere Experiment in Amazonia (LBA). A micrometeorological tower equipped with an eddy covariance system and instruments for meteorological variable measurements were used. The tower was located 2 km east of the Araguaia River (9°49′27.9″S, 50°08′92.8″W, 120 m in altitude), 1 km east of the Javaézinho River, at the northern border of the Bananal Island, and south of Cantão State Park. The Araguaia plains, where the Bananal Island is located, is characterized by an exuberant landscape comprising Cerrado and Amazon biomes extending throughout three conservation units: Araguaia National Park, Cantão State Park and the Cantão Environmental Protection Area. The Bananal Island encompasses a total area of 21,000 km^2 (approximately 80 km × 260 km) and is the largest fluvial island in the world, covered mainly by savannas and pastures with seasonal inundations occurring from February to June [3]. The instrumental fetch area covers different types of physiognomies: cerradão, semi deciduous forests (trees with an average height of 20 m), cerrado s.s. and bare field areas with isolated lagoons. The climate in the region is warm and wet, with mean annual precipitation of approximately 1466 mm year^{-1} and 90% of the total precipitation occurring in the wet season between October and April [3]. Measurements comprise the period from January 2004 to December 2006.
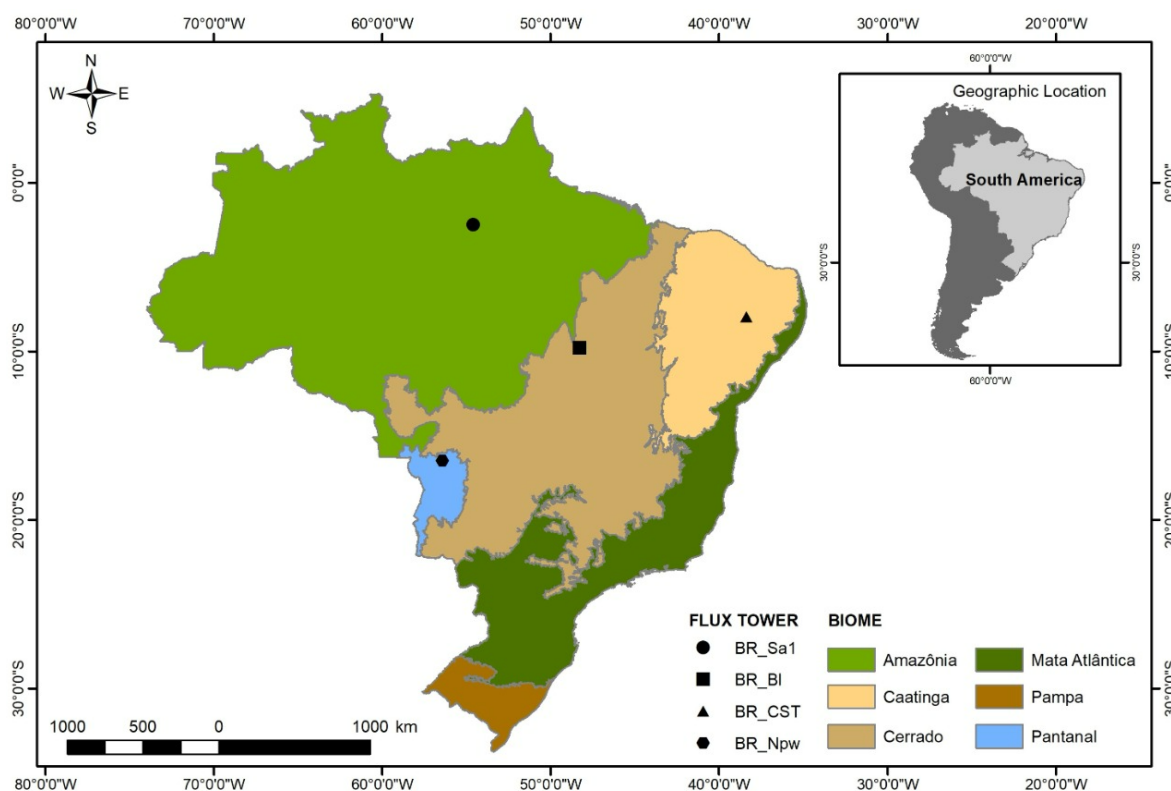
Figure 1. Location of the study sites with the native extension of each biome.

2.2.2. Caatinga Site

Measurements were carried out on a site managed by the Chico Mendes Institute for Biodiversity Conservation (ICMBio), and the micrometeorological tower is part of the NOWCDCB (National Observatory of Water and Carbon Dynamics in the Caatinga Biome, Figure 1) monitoring network. The campaign comprised the period from 1 January 2014 to 31 July 2015. The tower is located in a preserved Caatinga segment (BR-CST) within the Pajeú river watershed (7°58′05.20″S, 38°23′02.62″W, 430 m in altitude) in Serra Talhada city, Pernambuco state, Northeast Brazil. According to Köppen's classification, the climate is semiarid (BSwh), with summer rainfalls occurring between December and May (85% of total precipitation) as reported by [27]. Mean annual precipitation is approximately 640 mm, and average air temperatures range from 23.1 to 26.7 °C [27]. Native species at the site are *Mimosa hostilis*, *Mimosa verrucosa* and *Croton sonderianus*, while *Anadenanthera macrocarpa*, *Spondias tuberosa*, *Caesalpinia pyramidalis*, and *Ziziphus joazeiro* can also be found, with a mean height of 8.0 m [27]. Rainfall was provided by a "Instituto Nacional de Meteorologia" (INMET) station near of site.

2.2.3. Pantanal Site

The study was conducted at the Brazilian Northern Pantanal Wetland (BR-Npw) flux tower (Figure 1) located approximately 35 km SE of Pocone, Mato Grosso, Brazil (16°29′53.71″S: 56°24′45.91″W; 120 m altitude). The site is part of a research station managed by the Federal University of Mato Grosso (UFMT) within a national reserve managed by the Brazilian Social Service of Commerce (SESC Pantanal) [28,29]. According to Köppen classification, the regional climate is Aw, which is defined as a hot and wet climate with rainfall in the summer and dry in the winter [30]. The accumulated precipitation varies from 800 to 1500 mm/year [31,32]. The air temperature ranges between 29 and 32 °C (maximum) and between 17 and 20 °C (minimum) [33,34]. The soil type in the region is classified as Dystric Gleysol [35] with an average concentration of 429 g/kg of sand, 254 g/kg of silt, and 317 g/kg of clay, mean soil organic matter (SOM) (0–0.10 m depth) of 17 g/kg and a soil pH of 4.7 [36]. The vegetation of the site is typical of "scrub" forests in

the region, with a mean leaf area of 7.4 m^2 m^{-2} and a mean height of 6 m [37], dominated by *Combretum lanceolatum*, Phol (Combretaceae), a common species found on the riverbanks of the Pantanal region [38]. Vascular or semi-aquatic plants such as *Thalia geniculata* and *Nymphaea* sp. occur in more open areas [39]. These are dense forests that are referred to as "hyperseasonal" because they are subjected to both seasonal flooding and drought [40].

Our data were collected from 1 January 2015 to 31 December 2016. Micrometeorological variables were measured 20 m aboveground, close to the eddy covariance sensors. Air temperature (*Ta*, °C) and relative humidity (*RH*, %) were measured using a thermohygrometer (HMP45AC, Vaisala Inc., Woburn, MA, USA). Precipitation (*Ppt*, mm) was measured 2 m above the ground using a micrometeorological station (WXT520, Vaisala Inc., Helsinki, Finland) installed in an open area to avoid interception by the tower or tree canopy. The flood stage was determined by measuring water levels (*WL*) above the ground at the study site. These inundation levels (±1%) were measured along with water temperature (±0.3 °C) using a CTD-10 (Decagon Devices Inc., Pullman, WA, USA, ± 0.05% full scale at 20 °C) in 2015 and 2016. Due to instrument malfunction in 2014, the data for this year are not available. The start of each flood cycle began with the first reading of standing water at the site and ended when sensors indicated the absence of standing water. These flood cycles were then compared to the stage of the Cuiaba River collected by the RPPN-SESC Pantanal park rangers (pers. comm.) approximately 1 km away.

2.2.4. Amazon Site

Measurements were conducted on a site located at Tapajós National Forest (TNF, 2°51′S, 54°58′W, Figure 1), near the Santarém-Cuiabá highway (BR-163). The TNF is limited by the Tapajós River in the west and by the BR-163 highway in the east, extending 150 km to the south of Santarém city, Pará state. At the eastern side of the BR-163, the landscape is dominated by agriculture. The tower was installed approximately 6 km west of the highway. The canopy has a significant number of large emergent trees (to 55 m height), *Manilkara huberi* (Ducke) Chev., *Hymenaea courbaril* L., *Betholletia excelsa* Humb. and Bonpl., and *Tachigalia* spp., and a closed canopy at ~40 m [41]; this forest can be considered primary, or "oldgrowth" [42]. Analyzed data comprise CO_2 and energy fluxes and meteorological data. Measurements comprise daily and monthly means of hourly data in the period from January 2009 to December 2011. CO_2 fluxes were measured at 58 m in height through a closed-path analyzer (LICOR-6262) while a Campbell CSAT3 anemometer was used for tridimensional wind measurements. The 65 m micrometeorological tower is located at an area emerging from within the primary forest with a dense canopy of approximately 40 m in height, reaching up to 55 m for some emerging trees [43]. Rainfall was provided by a INMET station near of site (Belterra).

Figure 1 shows the location of the four studied sites and their respective biomes.

2.3. Instrumentation and Data Processing

Instrumentation in each of the sites is described in previous publications [3,27,44,45]. Gaps formed due to the exclusion of spurious data during the rigorous data screening process were filled using a marginal distribution sampling method (MDS) described by [46], which accounts for the covariance between fluxes and meteorological variables as well as the autocorrelation of fluxes. In this algorithm, three conditions are identified, and a procedure is adopted accordingly: (1) when flux data are missing, but meteorological data are available (Rg, Ta and VPD), missing data are replaced by the mean value in similar meteorological conditions over a seven-day window; (2) when only radiation data are available, the missing data are replaced by the mean value in similar meteorological conditions over a seven-day window; (3) when there are no meteorological data available, the missing data are replaced by the mean value in the last hour, thus accounting for the daily variability of each variable. If after these steps, data were still not filled, the procedure was repeated with larger window sizes until the gap could be filled. For the gap filling procedure, an automated online tool developed by the Max Planck Institute

for Biogeochemistry (http://www.bgc-jena.mpg.de/~MDIwork/eddyproc/, accessed on 2 February 2022) was used.

2.4. Flux Partitioning

Through CO_2 flux (NEE) partitioning, we obtained: gross primary production (GPP) and ecosystem respiration (R_{eco}). For the Cerrado and Pantanal sites, NEE is given as a proxy of the turbulent flow. At the other sites, NEE was composed of turbulent flow and storage. We used the flux partitioning method based on nighttime hours [46]. Since GPP = 0 at the nighttime period, NEE is given as:

$$NEE = R_{eco}, \text{ for nighttime hours} \tag{1}$$

$$NEE = R_{eco} - GPP, \text{ for daytime hours} \tag{2}$$

where R_{eco} (μmol m^{-2}s^{-2}) is the sum of autotrophic and heterotrophic respiration. R_{eco} and *GPP* were calculated using the online tool provided by the Max Planck Institute for Biogeochemistry (http://www.bgc-jena.mpg.de/~MDIwork/eddyproc/, accessed on 2 February 2022).

Diurnal corrections of missing NEE data were modeled based on daytime data using the common rectangular hyperbolic light-response curve model [47,48]:

$$NEE = \frac{\alpha \cdot \beta \cdot R_g}{\alpha \cdot R_g + \beta} + \gamma \tag{3}$$

where α (μmol C J^{-1}) is light-use efficiency and represents the initial slope of the light-response curve; β (μmol C m^{-2}s^{-1}) is the maximum CO_2 absorption rate of the canopy at light saturation; γ (μmol C m^{-2}s^{-1}) is ecosystem respiration and R_g (W m^{-2}) is global radiation. GPP was calculated as:

$$GPP = NEE + R_{eco} \tag{4}$$

To provide a better comparison with literature data (more in situ studies), we calculated Ecosystem WUE, calculated as:

$$WUE = GPP/ET \tag{5}$$

where ET (mm) is evapotranspiration.

2.5. MODIS Data

Remotely sensed GPP data obtained from the MODIS sensor onboard the Terra satellite were used. These data were calculated based on the concept of light use efficiency [47], through the relation between incident photosynthetically active radiation (PAR), the fraction of photosynthetically active radiation absorbed by plants (FPAR) and the actual light use efficiency (ε) of vegetation [49]:

$$GPP = \varepsilon * APAR \tag{6}$$

where APAR is the absorbed photosynthetically active radiation, which is calculated as the product between the FPAR—derived from the MOD15A2H product [50]—and the PAR. PAR values are obtained from the Global Modeling Assimilation Office (GMAO) reanalysis [51] set and correspond to 45% of the total incident solar energy in the visible spectrum (0.4 to 0.7 μm). In the MOD17A2 product, the values of ε are derived from the attenuation of its maximum value (εmax) due to two environmental stresses: (1) minimum temperature (Tmin), which can inhibit photosynthesis, reducing enzymatic activity, and (2) vapor pressure deficit (VPD), because high VPD can reduce stomatal conductance [52]. The GPP data for the Caatinga biome were derived from the MOD17A2 version 6.0 product [53] from the MODIS sensor on board the Terra satellite. This algorithm provides 8-day composite data in a 500 m spatial resolution.

Reanalysis data from the GMAO dataset (https://gmao.gsfc.nasa.gov/GMAO_products/reanalysis_products.php, accessed on 25 February 2022) used as input parameters for the MOD17A2 product were Tmin and VPD. Therefore, we carried out an overall assessment to check for inconsistencies in this dataset in relation to the same parameters measured at the Cerrado, Caatinga, Pantanal and Amazon biomes. FPAR and leaf area index (LAI) data from the MOD15A2H product were also verified. Furthermore, the MOD12 product [54] for land cover was also discussed regarding the years 2014 and 2015 in the region.

The MOD12 [54] product for land cover was also discussed regarding the Cerrado and Caatinga site for the period from 1 January 2014 to 31 July 2015, the Pantanal site for the period from 1 January 2015 to 31 December 2016, and the Amazon site from 1 January 2009 to 31 December 2011.

3. Results

3.1. Meteorological Conditions

Precipitation and air temperature data in all study sites (Figure 2), as well as daily observations of solar radiation, air temperature and relative humidity (Figure 3), presented a seasonality that was consistent with the local climatology. Highest radiation incidence was registered in the Caatinga and Pantanal sites, which makes them the warmest sites since air temperature is strongly correlated with solar radiation. The highest monthly temperature was found in the Pantanal site (Figure 2A), with 31.6 °C being registered in October, while the Amazon site presented the lowest temperatures (25.4 °C in April), which is also probably associated with the fact that radiation is lower (Figure 3A). The Caatinga and Pantanal sites are in phase regarding solar radiation (Figure 3A) and air temperature (Figure 3B) patterns, despite VPD values being three-fold higher in the Caatinga (Figure 3C), while VPD in the Pantanal is similar to that observed in the Amazon. VPD in the Amazon practically doubles until September, along with lower observed accumulated rainfall and higher air temperatures.
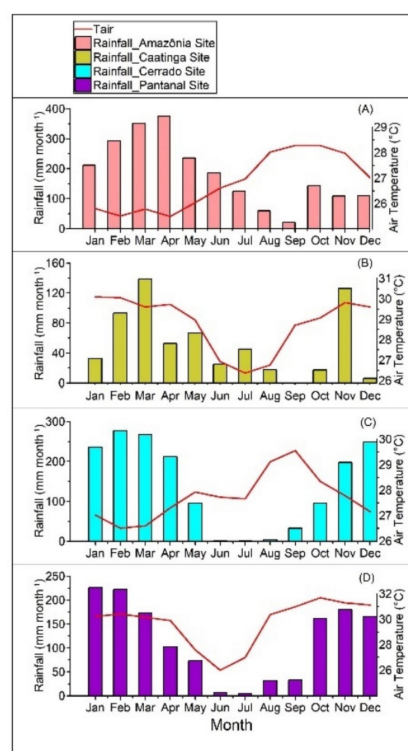
Figure 2. Monthly variation of mean air temperature (lines) and accumulated rainfall (bars) for each site and period: (**A**)—Amazonia: 2009–2011 (rainfall from INMET station); (**B**) Caatinga: January 2014−July 2015 (rainfall from INMET station); (**C**) Cerrado: 2004−2006; (**D**) Pantanal: 2015−2016).
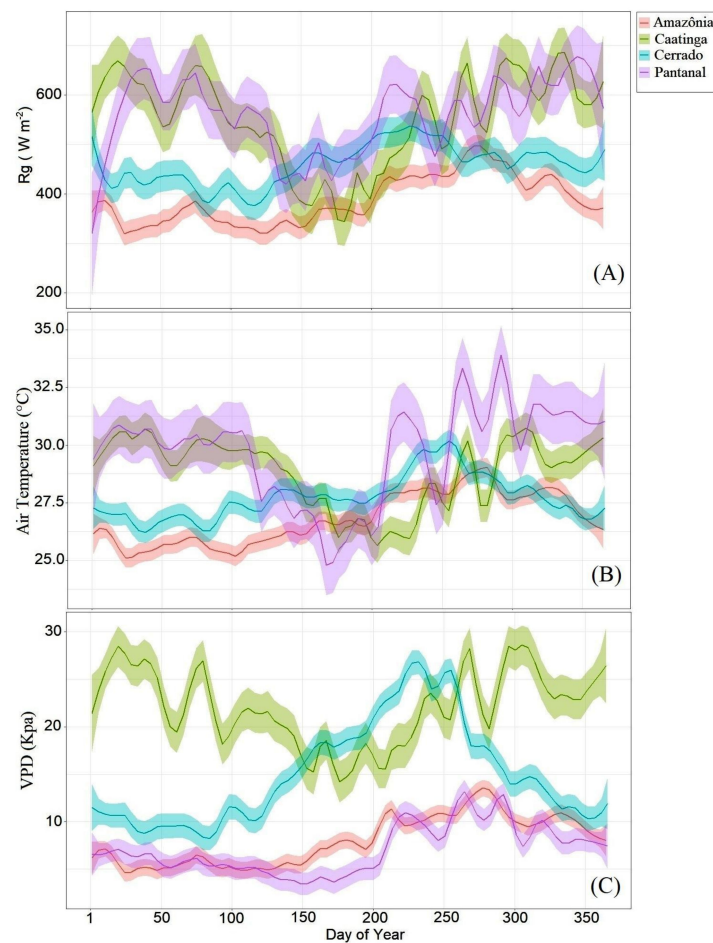
Figure 3. Seasonal variation of the daily mean of meteorological variables: (**A**) global incident radiation (W m^{-2}), (**B**) air temperature (°C) and (**C**) vapor pressure deficit (kPa). The shaded colored areas indicate data standard deviation.

Mean annual precipitation in the Amazon site was approximately 2221 mm, 38% higher than in the Pantanal site (1381 mm) and 25% higher than in the Cerrado site (1668 mm). Caatinga presented an annual accumulated rainfall value of 698.9 mm in 2014 and 376.3 mm until July 2015. The number of months with monthly precipitation <10% of total annual precipitation in each site (Figure 2) varied locally. In the Amazon, seven months met this criterion, while in the Cerrado and Pantanal, six months did as well. In the Caatinga, a total of nine months presented less than 10% of total annual rainfall. Besides the highest precipitation totals, the Amazon also presents the greatest monthly variability of precipitation, particularly in March (Figure 4). September is the month where precipitation in all four sites is the most similar, with the Caatinga site registering null precipitation and the other sites registering precipitation below 50 mm. In March, the difference between the wettest and the driest sites accounts for over 300 mm. Only in the months of June and July did the Caatinga site feature monthly accumulated rainfall higher than the Cerrado and Pantanal sites. Only the Amazon site surpassed 300 mm of precipitation in the months from February to April.
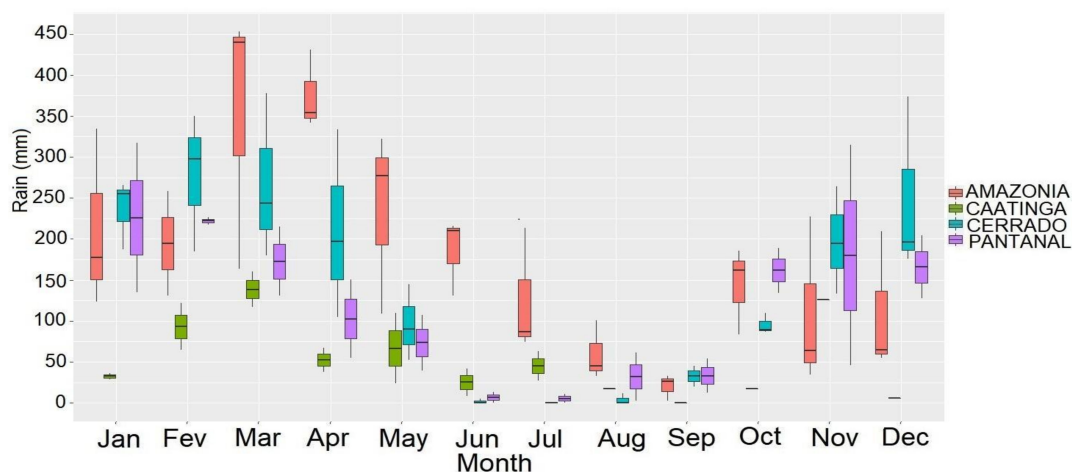
Figure 4. Monthly accumulated rainfall boxplots for each site and studied period (Amazonia: 2009–2011; Caatinga: January 2014−July 2015; Cerrado: 2004−2006; Pantanal: 2015−2016).

3.2. Water and Energy Fluxes

The annual cycle of observed daily ET (Figure 5) showed different patterns in the biomes: (1) Cerrado and Pantanal with maximum water vapor flux in October, decreasing toward March and April as the wet season ends; (2) a well-defined ET cycle in the Amazonia site, peaking in September during the dry season. ET cycles in the Cerrado and Pantanal are similar, with maximum daily ET of approximately 7.0 mm day^{-1}. In July, daily ET values are similar in the Cerrado, Pantanal and Amazon sites, with a similar pattern to what was previously observed for solar radiation and air temperature (Figure 3A,B). The Caatinga site stood out, with values down to three-fold lower if compared to the other sites, despite the similar seasonal pattern (higher daily ET between October and April, lower daily ET between May and September). Maximum ET coincides with higher energy availability (radiation) and higher temperatures in the sites, between October and November.
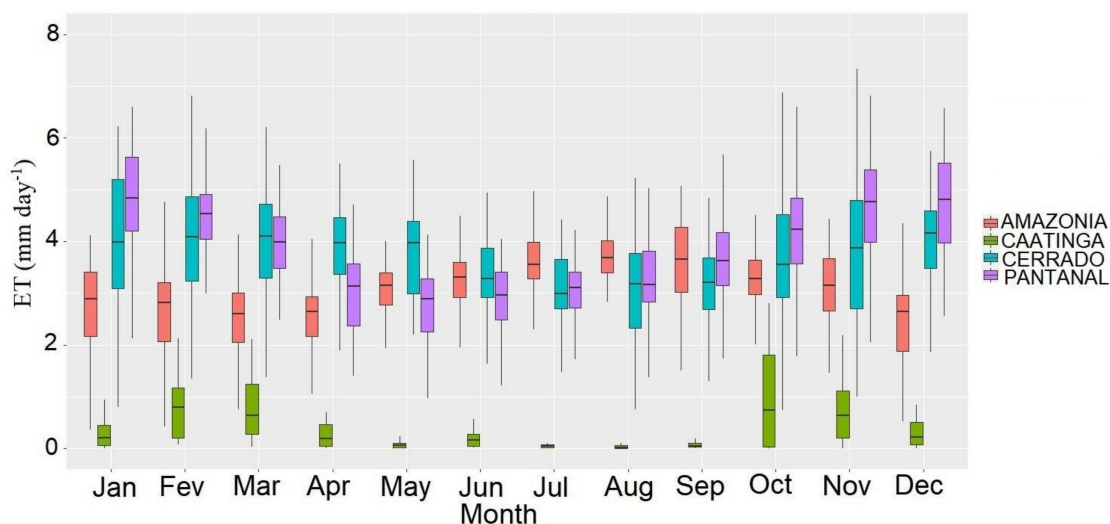
Figure 5. Monthly daily evapotranspiration (mm day^{-1}) boxplots for each site and studied period (Amazonia: 2009−2011; Caatinga: January 2014−July 2015; Cerrado: 2004−2006; Pantanal: 2015−2016).

The monthly seasonal patterns of net radiation and sensible and latent heat fluxes differ strongly from site to site. In the Pantanal, Caatinga and Cerrado, net radiation (Rn) presents values higher than 120 W m^{-2} (Figure 6A) in January and May, with a decreasing pattern the following months. The Amazon site, located further north than the other sites

and therefore more influenced by the Intertropical Convergence Zone during these months, presented lower values, of approximately 100 W m^{-2}, with increasing values from May until the peak of the dry season in September. Hourly Rn patterns are similar, with the Amazon site featuring approximately 50 W m^{-2} less than the other sites. However, latent heat flux (LE) (Figure 6B) and sensible heat flux (H) (Figure 6C) have distinct hourly and monthly patterns. Maximum LE in the Pantanal is three-fold higher than in the Caatinga, while the H pattern is the inverse. Rn, H and LE patterns are in phase regarding Pantanal and Amazonia sites, particularly because LE and H sharply increase in the dry season, following the increase in available energy. An opposite relationship is found between Rn and LE in the Cerrado and Caatinga sites, which increase in September and October while LE reduces in the same period.
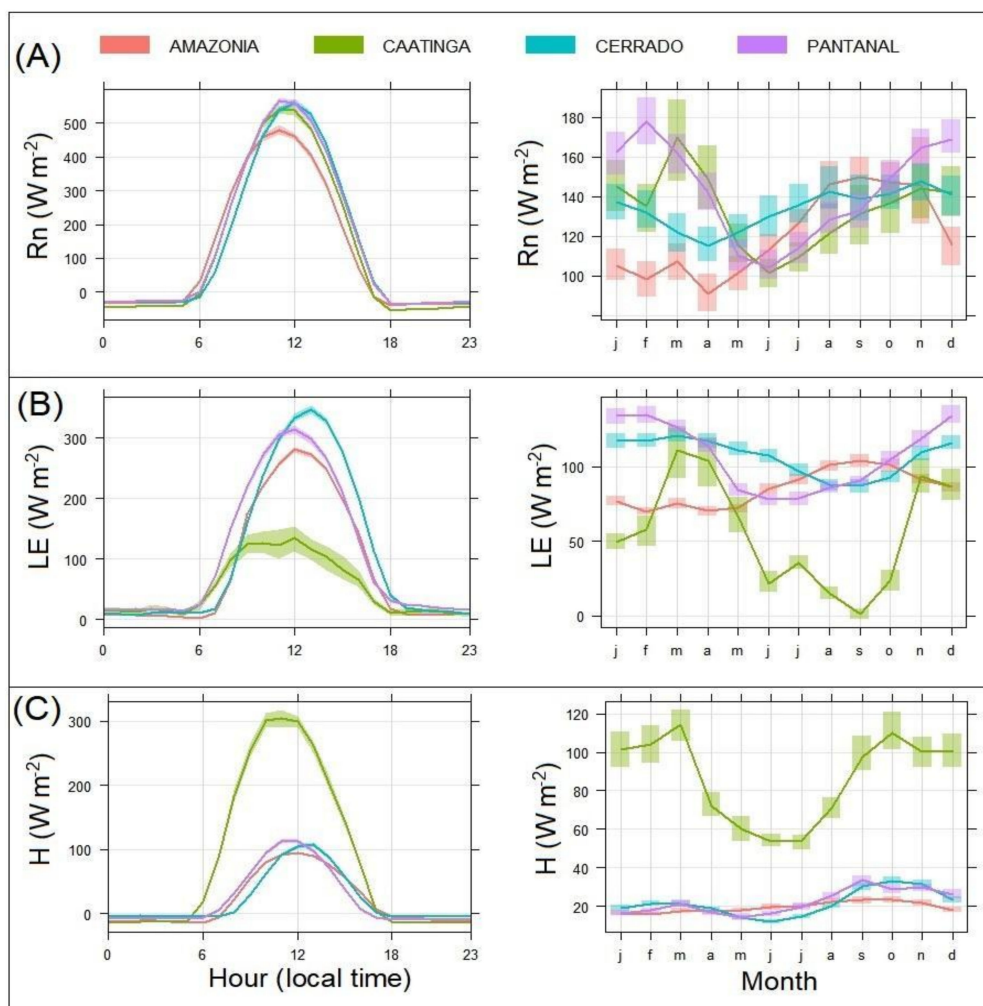
Figure 6. Hourly and monthly variation of energy fluxes: (**A**) net radiation (Rn, W m^{-2}), (**B**) latent heat flux (LE, W m^{-2}) and (**C**) sensible heat flux (H, W m^{-2}).

3.3. Carbon Fluxes and WUE

According to the daily GPP analysis shown in Figure 7, seasonal changes in GPP are more intense in the Caatinga and Pantanal sites if compared to the Amazonia and Cerrado sites. The coefficient of determination (R^2) between observed GPP and evapotranspiration (Figure 8) was also higher in the Caatinga and Pantanal. Maximum values reach up to 9.0 gC m^{-2} d^{-1} in the Cerrado and Amazonia, while the lowest GPP values reach approximately 0.5 gC m^{-2} d^{-1} in the Caatinga. The seasonality and intensity of GPP values in the Amazon and Cerrado are similar, while in the Caatinga and Pantanal, they are similar only between June and July. Regarding maximum values, GPP peaks in April in the Cerrado, coinciding

with the period of least radiation availability after the site inundation, while in the Amazon, GPP peaks in October, characterized by high radiation, air temperature and an increase in precipitation after an annual minimum in September.
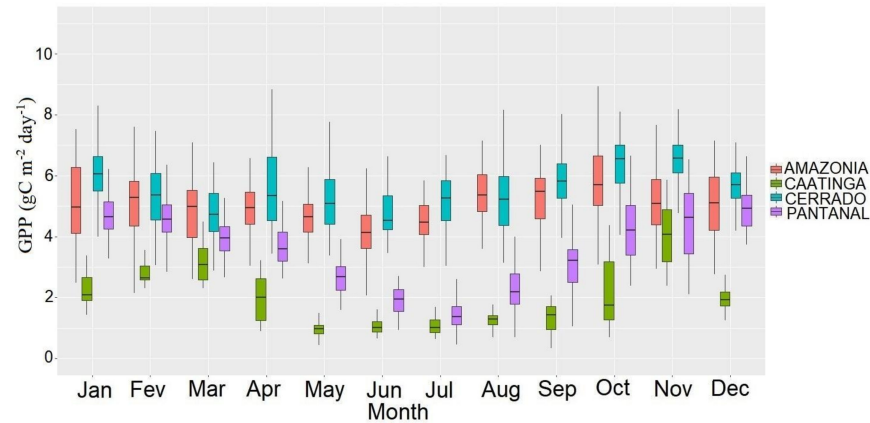
Figure 7. Monthly GPP (gC m^{-2} day^{-1}) boxplot for each site and study period (Amazonia: 2009−2011; Caatinga: January 2014−July 2015; Cerrado: 2004−2006; Pantanal: 2015−2016).
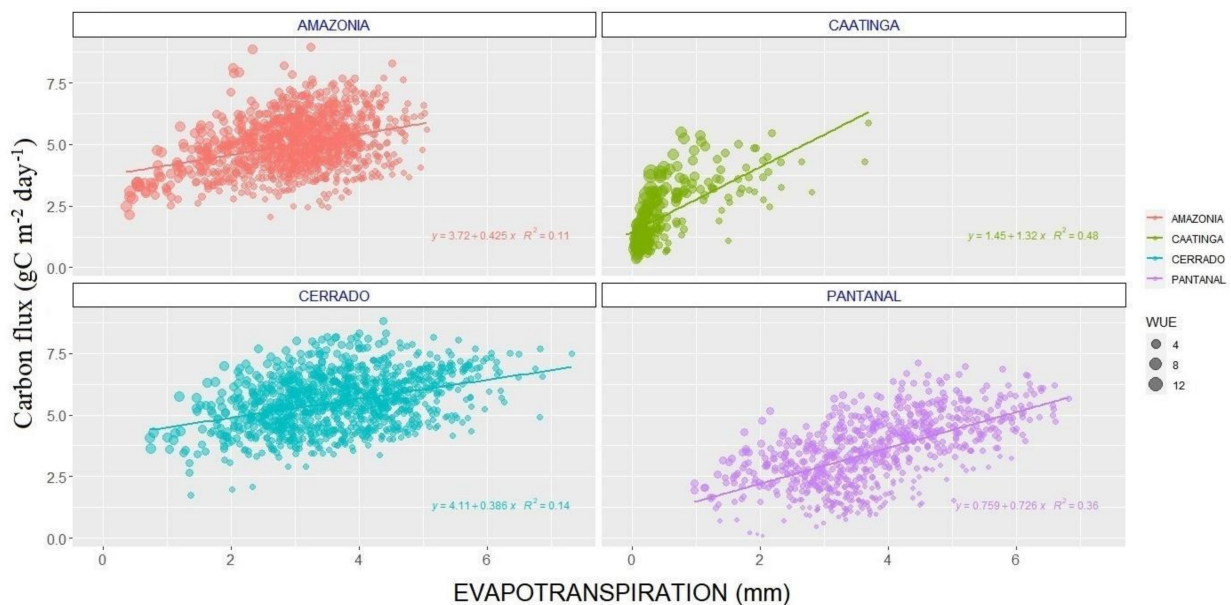
Figure 8. Correlation between daily GPP averages and evapotranspiration for each site. The size of the circles indicates the intensity of water-use efficiency (WUE) estimated at each day (gC kg H$_2$O day^{-1}).

We also assessed observed GPP data by comparing them with MODIS satellite data on a monthly scale (Figure 9). Results show a high overestimation of satellite data in drier periods, especially in the Amazonia site (Figure 9A). In the Caatinga site (Figure 9B), measurements are more similar from September to November if we consider the median values and monthly variability. In the Cerrado site (Figure 9C), MODIS GPP underestimates observed data in the dry season (August and September), while in the Pantanal (Figure 9D), daily variability of MODIS data is much more prominent than observed data, despite the coherence in representing the seasonal cycle. Given these patterns, the best correlations were found in the Pantanal (R^2 = 0.31) and Caatinga (R^2 = 0.27) sites (Figure 10), with values similar to what is found in the general literature regarding MODIS GPP assessment (Table 1). Due to the importance of investigating specific local water cycles and the effect of drought on the water balance and carbon uptake, we calculated WUE (Figure 11), showing interesting variability aspects depending on the studied biome. WUE is lower in the site

with the highest evapotranspiration (Pantanal), while a remarkable variability and the highest WUE values are found in the Caatinga site. WUE in the other sites did not present great seasonal differences, with values reaching approximately 4.0 gC kg H_2O day^{-1} in the driest months (between September and October). WUE surpassed 15 gC kg H_2O day^{-1} in the driest month (September) of the driest site (Caatinga), sharply decreasing in October with the occurrence of rainfall. Mean annual WUE values estimated in this study delineate new thresholds if compared to previously reported values in the literature (Table 2), with the Pantanal site featuring WUE lower than 1.0 gC kg H_2O year^{-1} and the Caatinga site featuring values near 5.8 gC kg H_2O year^{-1}, which is much higher than in other dry forests studied in the literature.
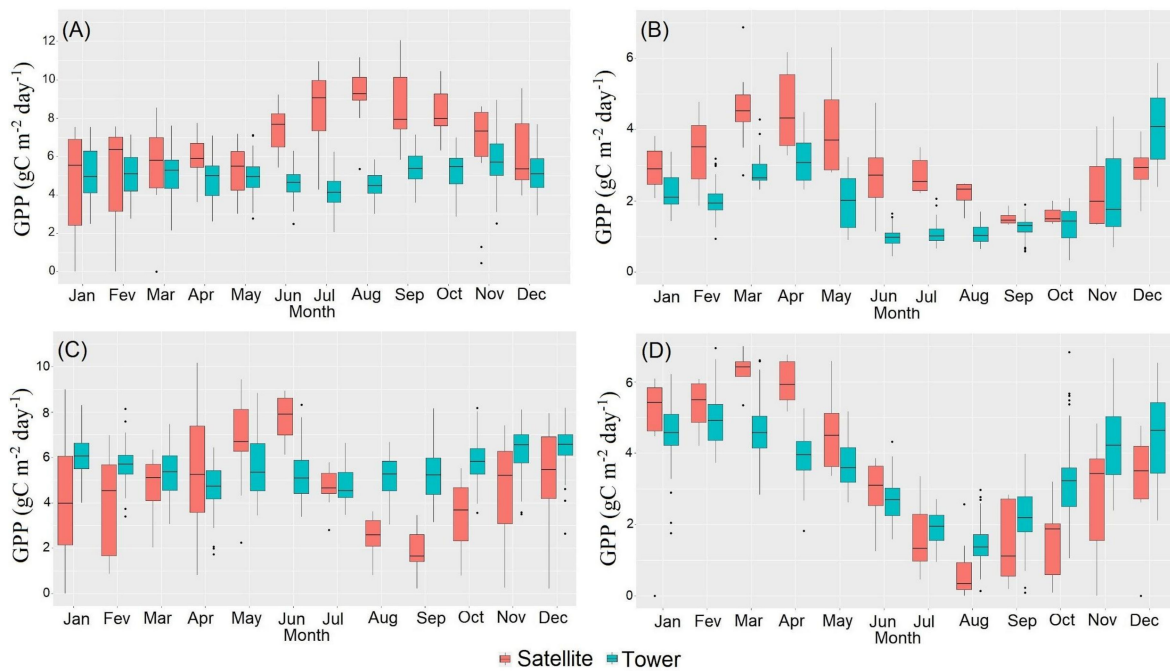
Figure 9. Monthly GPP boxplot (gC m^{-2} day^{-1}) for eddy covariance observed data (Tower) and MODIS—derived data (Satellite) for the: (**A**) Amazonia; (**B**) Caatinga; (**C**) Cerrado; (**D**) Pantanal sites.
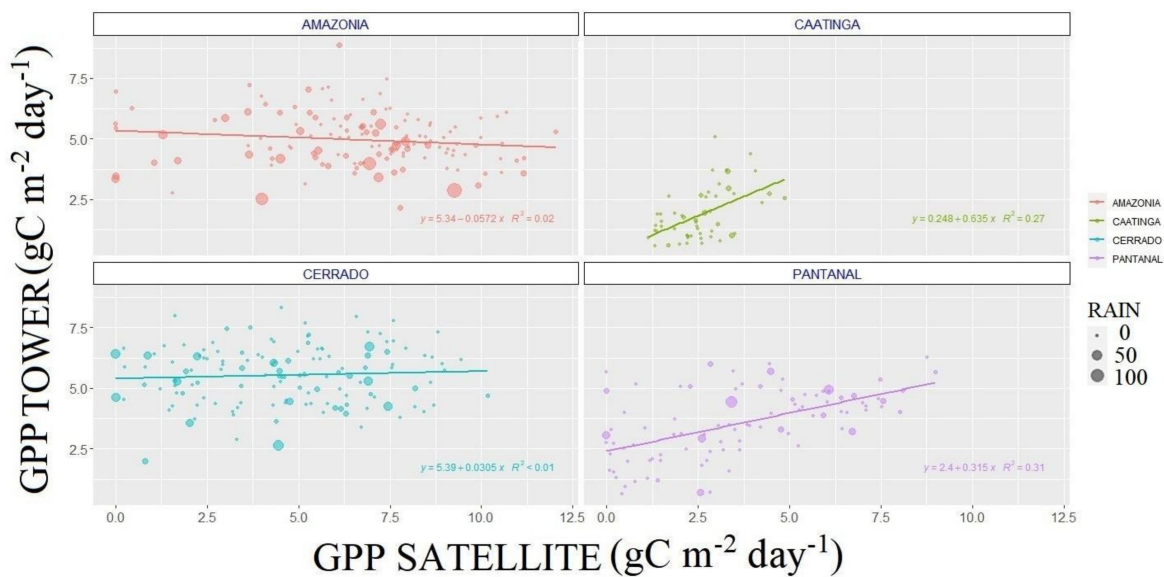
Figure 10. Correlation between daily tower GPP $\times$ MODIS GPP for each site. The size of the circles indicates the intensity of daily accumulated rainfall (mm).

Table 1. Statistical summary of studies comparing MODIS GPP and eddy covariance estimations for different land covers using linear regression models.

Forest Type	Slope	R^2	Reference
Alpine grassland	1.30	0.50	Zhu et al. [55]
Alpine grassland	0.58	0.17	Zhu et al.
Dry tropical forest	0.24	0.27	**This study**
Floodplain forest	5.39	0.01	**This study**
Primary forest	5.34	0.02	**This study**
Semi-deciduous forest	0.49	0.32	Danelichen et al. [56]
Temperate grassland	1.59	0.70	Zhu et al., 2018
Temperate grassland	0.50	0.40	Zhu et al., 2018
Tropical grassland	0.89	0.53	Zhu et al., 2018
Tropical peatland	0.23	0.16	Wang et al. [57]
Tropical grassland	0.91	0.63	Zhu et al., 2018
Tropical grassland	0.89	0.53	Zhu et al., 2018
Wetland	2.40	0.31	**This study**
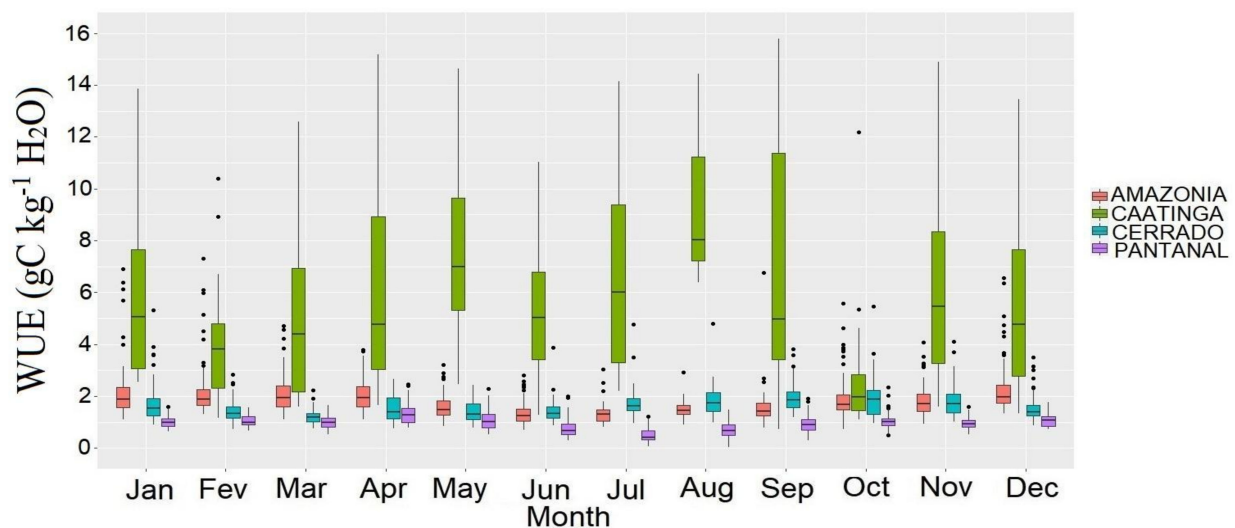
Figure 11. Monthly WUE (gC kg H_2O day^{-1}) boxplot for each site and studied period: (Amazonia: 2009−2011; Caatinga: 01/2014−07/2015; Cerrado: 2004−2006; Pantanal: 2015−2016).

Table 2. Comparison between mean annual WUE retrieved in the present study with values for different types of forests found in the literature.

Forest Types	WUE (g C kg^{-1}H$_2$O)	References
Wetland	0.95	**This study**
Boreal treeless wetland	1.2	Kuglitsch et al. [58]
Floodplain forest	1.61	**This study**
Maritime pine	1.69	Berbigier et al. [59]
Primary forest	1.82	**This study**
Deciduous broadleaf forest	1.87	Wang et al.
Old-growth forest	1.83	Liu et al. [60]
Evergreen broadleaf forest	2.35	Tang et al. [61]
Conifer plantation forest	2.53	Yu et al. [62]
Deciduous broadleaf forest	2.57	Yu et al.
Eucalypt plantation	2.87	Rodrigues et al. [63]
Ponderosa pine	2.97	Law et al. [64]
Evergreen broadleaf forest	3.13	Tang et al.
Boreal aspen	3.70	Krishnan et al. [65]

Table 2. *Cont.*

Forest Types	WUE (g C kg^{-1}H$_2$O)	References
Temperate broad-leaved deciduous	5.0	Kuglitsch et al.
Douglas-fir	5.40	Ponton et al. [66]
Dry tropical forest	5.79	**This study**

4. Discussion

Evapotranspiration showed well-defined seasonality in all sites, varying at the annual scale with local precipitation, radiation availability and increasing temperatures. Highest evapotranspiration values were registered in the warmer months and/or in months with more radiation or precipitation. Evapotranspiration reached maximum values in the Cerrado and Pantanal sites in wetter months, reaching up to 7 mm day^{-1} in November, with a mean value slightly above 3 mm day^{-1}. In the Caatinga site, even in the month with the highest evapotranspiration rates (October), overall values did not reach the same intensity of the other sites, showing the particularity of this site regarding its arid climate (BSh) according to Köppen's classification (Liang et al., 2020) [67]. Crucial studies have already been conducted to estimate the magnitude, seasonality and controls of ET at the local scale using eddy covariance measurements in Brazil (Da Rocha et al., 2009; Costa et al., 2010) [6,68]. These studies usually show that dry season evapotranspiration is higher than in the wet season, and Rn is the main ET control in tropical rainforests (such as the Amazon), while it is not true for the Caatinga, Cerrado and Pantanal sites. Our results showed that in these sites, evapotranspiration decreases throughout the dry season, reaching the lowest rates between August and September, when the Amazon features its highest values. Even during the dry season, high evapotranspiration rates can be explained by the predominance of pioneer tree species (*Combretum lanceolatum* and *Vochysia divergens*) with high photosynthesis rates and stomatal conductance (gs) (Dalmagro et al., 2013; 2016) [69,70], associated with the ability of these species to extract water from deep storages containing similar water content to that of inundation areas and wet periods (Sanches et al., 2011; Vourlitis et al., 2011; Dalmagro et al., 2013; da Silva et al., 2021) [29,69,71,72].

In the dry season of the Cerrado site, an inverse relationship was found between LE and Rn, which is typical of savanna ecosystems, where the root system does not reach deep water storages, but part of the vegetation is adapted and relies on senescence mechanisms of tree leaves and dormancy of grasses (3). A pulse in productivity (increased GPP) that is directly related to the increase in water availability (rainfall) can be observed, particularly from October on, which marks the beginning of the transition from the dry to the wet season. As expected, all sites reduced productivity in response to increased rainfall variability, with the most productive ecosystems being those with the highest precipitation rates (Amazon and Cerrado). The low rainfall rates observed in the Caatinga in October were sufficient to drive a sharp increase in productivity, which indicates that more frequent rainfall events in this environment could lead to more nutrient availability and the mitigation of water stress through leaf absorption mechanisms. A further indicator of these aspects can be observed through the remarkable variability in evapotranspiration during this month in the Caatinga. Furthermore, this biome presented the best correlations between GPP and evapotranspiration. The comparison between observed and remotely sensed data showed that both datasets represent the same seasonality, despite their weak correlation. Satellite data accurately represents the strong response of the Pantanal and Caatinga sites to local precipitation, while the results are not satisfactory regarding the dry period in the Amazon and Cerrado. The weak correlation between GPP data in tropical forests is well documented (Zhu et al., 2018) [55] and is generally attributed to light-use efficiency, which is underestimated by the MODIS GPP algorithm (Sjöström et al., 2013) [73]. Additionally, potential uncertainties regarding the FPAR might also affect MODIS GPP estimates, which have also been discussed in the literature (Liu et al., 2017) [60]. Despite its wide use, our results corroborate previous studies reporting the need to use MODIS GPP data with

caution for interannual and intra-annual studies, as suggested by Zhu et al. [55]. Our study revealed that humid biomes present lower WUE, and drier biomes present higher WUE, with decreasing values with the onset of the wet season and maximum values in the dry season. This result is consistent with previous studies in other environments (Liu et al., 2017; Singh et al., 2014; Yu et al., 2008) [60,62,74]. Ito and Inatomi [75] claim that forest ecosystems presented WUE values comparable or superior to arid (such as caatinga) and shrub biomes (such as Cerrado and Pantanal), with an intermediate value of 0.6–1.2 g C kg^{-1} H$_2$O for humid forest biomes. The average WUE for the Pantanal is within this range.

WUE responds differently to seasonal water availability in each biome. Overall, more productive biomes present high WUE (Xue et al., 2015) [76]. In sparsely vegetated areas, such as the Cerrado (savannas) and the Pantanal wetlands, WUE varies greatly throughout the year, despite presenting lower values than the Caatinga. From January to April, when precipitation is high in all sites (except Caatinga), the Amazon site featured an increase in WUE daily values, while the Cerrado WUE decreased, and the Pantanal WUE remained unaltered. From May, rainfall triggers a sharp decrease in WUE over these regions until September. Our results reveal important implications for the understanding of climate change effects on carbon and water exchange processes in tropical biomes, because the projected reduction in water availability over these sites due to the increasing number of dry days [77] may lead to an increase in WUE at the ecosystem level. However, increasing temperatures may further increase or reduce ecosystem WUE at the monthly scale. Consequently, changes in ecosystem WUE due to climate change will depend on the relative impact of these changes in precipitation and temperature. Caatinga WUE is highly dependent on water availability, with lower values and variability in the wetter months and higher values and variability in the drier months. The results found here corroborate other studies in other parts of the Caatinga biome [78–82], and it is important to report that owing to measurement difficulties, few studies have systematically compared global patterns of WUE of terrestrial ecosystems across different biomes or have analyzed the seasonal variability of WUE in relation to weather conditions, because ecosystem WUE is slightly different from plant WUE [61]. Plant physiologists consider WUE at leaf or stand scales and are mainly interested in relations between total or above-ground biomass, stem biomass or net CO$_2$ uptake to transpiration or evapotranspiration (ET), and although uncertainties associated with site-to-site variation in site quality criteria, flux measurement methods, calculations and data quality control still exist, ongoing standardization and quality assurance efforts enable global integration with other tools [61].

5. Conclusions

In this study, we presented data on the seasonal variations of energy fluxes, climatic variables, GPP, ET and WUE for different tropical biomes in Brazil. Furthermore, correlations between observed carbon exchange data and remotely sensed data were also assessed. Results showed that GPP and ET responses to meteorological variables (solar radiation, air temperature, precipitation and VPD) are in phase, suggesting that this meteorological variability controls photosynthesis and ET in a similar fashion on a monthly scale, despite both direct and inverse relationships having been found depending on the type of environment. Based on our results, our study concludes that inconsistent MODIS GPP estimates for some months and sites indicate that the parametrizations used in the MOD17A2H GPP algorithm (such as FPAR) may need to be enhanced over certain land covers in order to improve estimates. WUE in the studied sites varied annually from 0.95 to 5.79 gC kg^{-1} H$_2$O, with minimum and maximum values differing from usually found values for other environments worldwide. This study will aid future studies regarding the influence of global warming and water stress on carbon and water fluxes in similar tropical forests.

References

1. Andreae, M.O.; Artaxo, P.; Brandão, C.; Carswell, F.E.; Ciccioli, P.; da Costa, A.L.; Culf, A.D.; Esteves, J.L.; Ash, J.H.C.; Grace, J.; et al. Biogeochemical cycling of carbon, water, energy, trace gases, and aerosols in Amazonia: The LBA-EUSTACH experiments. *J. Geophys. Res.* **2002**, *107*, 25. [CrossRef]
2. Araújo, A.C.; Nobre, A.D.; Kruijt, B.; Elbers, J.A.; Dallarosa, R.; Stefani, P.; Randow, C.; von Manzi, A.O.; Culf, A.D.; Gash, J.H.C.; et al. Comparative measurements of carbon dioxide fluxes from two nearby towers in a central Amazonian rainforest: The Manaus LBA site. *J. Geophys Res.* **2002**, *107*, 8090. [CrossRef]
3. Borma, L.D.S.; da Rocha, H.R.; Cabral, O.M.; von Randow, C.; Collicchio, E.; Kurzatkowski, D.; Brugger, P.J.; Freitas, H.; Tannus, R.; Oliveira, L.; et al. Atmosphere and hydrological controls of the evapotranspiration over aflood plain forestin the Bananal Island region, Amazonia. *J. Geophys. Res.-Biogeo.* **2009**, *114*, G01003. [CrossRef]
4. Carswell, F.E.; Costa, A.L.; Palheta, M.; Malhi, Y.; Meir, P.; Costa, J.d.P.R.; Ruivo, M.d.L.; Leal, L.d.S.M.; Costa, J.M.N.; Clement, R.J.; et al. Seasonality in CO2 and H2O flux at an eastern Amazonian rain forest. *J. Geophys. Res.* **2002**, *107*, 16.
5. Rocha, H.R.; Goulden, M.L.; Miller, S.D.; Menton, M.C.; Pinto, L.D.V.O.; De Freitas, H.C.; E Silva Figueira, A.M. Seasonality of water and heat fluxes over a tropical forest in Eastern Amazonia. *Ecol. Appl.* **2004**, *14*, 22–32. [CrossRef]
6. Rocha, H.R.; Manzi, A.O.; Cabral, O.M.; Miller, S.D.; Goulden, M.L.; Saleska, S.R.; Restrepo-Coupe, N.; Wofsy, S.C.; Borma, L.S.; Artaxo, P.; et al. Patterns of water and heat flux across a biome gradient from tropical forest to savanna in Brazil. *J. Geophys. Res.* **2009**, *114*, 8. [CrossRef]
7. Sellers, P.J.; Shuttleworth, W.J.; Dorman, J.L.; Dalcher, A.; Roberts, J.M. Calibrating the Simple Biosphere Model for Amazonian tropical forest using field and remote sensing data. Part I: Average calibration with field data. *J. Appl. Meteorol.* **1989**, *28*, 727–759.
8. Saad, S.I.; da Rocha, H.R.; Silva Dias, M.A.F.; Rosolem, R. Can the deforestation breeze change the rainfall in Amazonia? A case study for the BR-163 highway region. *Earth Interact.* **2010**, *14*, 1–25. [CrossRef]
9. Bai, Y.; Li, X.; Zhou, S.; Yang, X.; Yu, K.; Wang, M.; Liu, S.; Wang, P.; Wu, X.; Wang, X.; et al. Quantifying plant transpiration and canopy conductance using eddy flux data: An underlying water use efficiency method. *Agric. For. Meteorol.* **2019**, *271*, 375–384. [CrossRef]
10. Mendes, K.R.; Campos, S.; Mutti, P.R.; Ferreira, R.R.; Ramos, T.M.; Marques, T.V.; dos Reis, J.S.; de Lima Vieira, M.M.; Silva, A.C.N.; Marques, A.M.S.; et al. Assessment of SITE for CO2 and Energy Fluxes Simulations in a Seasonally Dry Tropical Forest (Caatinga Ecosystem). *Forests* **2021**, *12*, 86. [CrossRef]
11. Ruhoff, A.L.; Paz, A.R.; Collischonn, W.; Aragao, L.E.O.C.; Rocha, H.R.; Malhi, Y.S. A MODIS-Based Energy Balance to Estimate Evapotranspiration for Clear-Sky Days in Brazilian Tropical Savannas. *Remote Sens.* **2012**, *4*, 703–725. [CrossRef]

12. Nascimento, G.S.; Ruhoff, A.; Cavalcanti, J.R.; Marques, D.M.; Roberti, D.R.; da Rocha, H.R.; Munar, A.M.; Fragoso, C.R.; de Oliveira, M.B.L. Assessing CERES Surface Radiation Components for Tropical and Subtropical Biomes. *IEEE J. Sel. Top. Appl. Earth Obs. Remote Sens.* **2019**, *1*, 3826–3840. [CrossRef]

13. Fonseca, L.D.M.; Dalagnol, R.; Malhi, Y.; Rifai, S.W.; Costa, G.B.; Silva, T.S.F.; da Rocha, H.R.; Tavares, I.B.; Borma, L.S. Phenology and Seasonal Ecosystem Productivity in an Amazonian Floodlain Forest. *Remote Sens.* **2019**, *11*, 1530. [CrossRef]

14. Moreira, A.A.; Ruhoff, A.L.; Roberti, D.R.; de Arruda Souza, V.; da Rocha, H.R.; Paiva, R.C.D. Assessment of terrestrial water balance using remote sensing data in South America. *J. Hydrol.* **2019**, *575*, 131–147. [CrossRef]

15. Myneni, R.; Knyazikhin, Y.; Park, T. MCD15A3H MODIS/Terra+Aqua Leaf Area Index/FPAR 4-Day L4 Global 500m SIN Grid V006. NASA EOSDIS Land Processes DAAC. Available online: https://lpdaac.usgs.gov/products/mcd15a3hv006/ (accessed on 26 April 2022).

16. Laipelt, L.; Ruhoff, A.L.; Fleischmann, A.S.; Kayser, R.H.B.; Kich, E.M.; da Rocha, H.R.; Neale, C.M.U. Assessment of an Automated Calibration of the SEBAL Algorithm to Estimate Dry-Season Surface-Energy Partitioning in a Forest–Savanna Transition in Brazil. *Remote Sens.* **2020**, *12*, 1108. [CrossRef]

17. Ferreira, R.R.; Mutti, P.R.; Mendes, K.R.; Campos, S.; Marques, T.V.; Oliveira, C.P.; Gonçalves, W.; Mota, J.; Difante, G.; Urbano, S.A.; et al. An assessment of the MOD17A2 gross primary production product in the Caatinga biome, Brazil. *Int. J. Remote Sens.* **2021**, *42*, 1275–1291. [CrossRef]

18. Fei, X.H.; Jin, Y.Q.; Zhang, Y.P.; Sha, L.Q.; Liu, Y.T.; Song, Q.H.; Zhou, W.; Liang, N.; Yu, G.; Zhang, L.; et al. Eddy covariance and biometric measurements show that a savanna ecosystem in Southwest China is a carbon sink. *Sci. Rep.* **2017**, *7*, 41025. [CrossRef]

19. Kanniah, K.D.; Beringer, J.; Hutley, L.B. Environmental controls on the spatial variability of savanna productivity in the Northern Territory, Australia. *Agric. For. Meteorol.* **2011**, *151*, 1429–1439. [CrossRef]

20. Quansah, E.; Mauder, M.; Balogun, A.A.; Amekudzi, L.K.; Hingerl, L.; Bliefernicht, J.; Kunstmann, H. Carbon dioxide fluxes from contrasting ecosystems in the Sudanian Savanna in West Africa. *Carbon Balance Manag.* **2015**, *10*, 1. [CrossRef]

21. Scheiter, S.; Higgins, S.I.; Beringer, J.; Hutley, L.B. Climate change and long-term fire management impacts on Australian savannas. *New Phytol.* **2015**, *205*, 1211–1226. [CrossRef]

22. Scott, R.L.; Hamerlynck, E.P.; Jenerette, G.D.; Moran, M.S.; Huxman, T.E.; Barron-Gafford, G.A. Carbon dioxide exchange in a semidesert grassland through drought-induced vegetation change. *J. Geophys. Res.* **2010**, *115*, G03026. [CrossRef]

23. Davidson, E.A.; de Araújo, A.C.; Artaxo, P.; Balch, J.K.; Brown, I.F.; Bustamante, M.M.; Coe, M.T.; DeFries, R.S.; Keller, M.; Longo, M.; et al. The Amazon basin in transition. *Nature* **2012**, *481*, 321–328. [CrossRef] [PubMed]

24. WMO. WMO Greenhouse Gas Bulletin (GHG Bulletin)—No.15: The State of Greenhouse Gases in the Atmosphere Based on Global Observations through 2018. 2019. Available online: https://library.wmo.int/doc_num.php?explnum_id=10437 (accessed on 27 March 2022).

25. Flux Tower BR-Sa1. Available online: https://ameriflux.lbl.gov/sites/siteinfo/BR-Sa1 (accessed on 1 February 2022).

26. Flux Tower BR-CST. Available online: https://ameriflux.lbl.gov/sites/siteinfo/BR-CST (accessed on 1 February 2022).

27. Flux Tower BR-Npw. Available online: https://ameriflux.lbl.gov/sites/siteinfo/BR-Npw (accessed on 1 February 2022).

28. Alcântara, L.R.P.; Coutinho, A.P.; dos Santos Neto, S.M.; Carvalho de Gusmão da Cunha Rabelo, A.E.; Antonino, A.C.D. Modeling of the Hydrological Processes in Caatinga and Pasture Areas in the Brazilian Semi-Arid. *Water* **2021**, *13*, 1877. [CrossRef]

29. Dalmagro, H.J.; Zanella de Arruda, P.H.; Vourlitis, G.L.; Lathuilliere, M.J.; de Nogueira, S.J.; Couto, E.G.; Johnson, M.S. Radiative forcing of methane fluxes offsets net carbon dioxide uptake for a tropical flooded forest. *Glob. Change Biol.* **2019**, *25*, 1967–1981. [CrossRef]

30. Da Silva, J.B.; Valle Junior, L.C.G.; Faria, T.O.; Marques, J.B.; Dalmagro, H.J.; Nogueira, J.S.; Vourlitis, G.L.; Rodrigues, T.R. Temporal Variability in Evapotranspiration and Energy Partitioning over a Seasonally Flooded Scrub Forest of the Brazilian Pantanal. *Agric. For. Meteorol.* **2021**, *308*, 108559. [CrossRef]

31. Alvares, C.A.; Stape, J.L.; Sentelhas, P.C.; de Moraes Gonçalves, J.L.; Sparovek, G. Köppen's climate classification map for Brazil. *Meteorol. Z.* **2013**, *22*, 711–728. [CrossRef]

32. Fantin-Cruz, I.; Girard, P.; Zeilhofer, P.; Collischonn, W.; da Cunha, C.N. Unidades fitofisionômicas em mesoescala no Pantanal Norte e suas relações com a geomorfologia. *Biota Neotropica* **2010**, *10*, 31–38. [CrossRef]

33. Johnson, M.S.; Couto, E.G.; Pinto, O.B.; Milesi, J.; Santos Amorim, R.S.; Messias, I.A.M.; Biudes, M.S. Soil CO2 Dynamics in a Tree Island Soil of the Pantanal: The Role of Soil Water Potential. *PLoS ONE* **2013**, *8*, e64874. [CrossRef]

34. Rodrigues, T.R.; Curado, L.F.A.; Novais, J.W.Z.; de Oliveira, A.G.; de Paulo, S.R.; Nogueira, D.S. Distribuição sazonal dos componentes do balanço de energia no norte do Pantanal. *Rev. Ciências Agro-Ambient.* **2011**, *9*, 165–175.

35. Biudes, M.S.; Machado, N.G.; Danelichen, V.H.d.M.; Souza, M.C.; Vourlitis, G.L.; Nogueira, J.d.S. Ground and remote sensing-based measurements of leaf area index in a transitional forest and seasonal flooded forest in Brazil. *Int. J. Biometeorol.* **2014**, *58*, 1181–1193. [CrossRef]

36. Couto, E.; Klinger, P.; Jacomine, T.; Nunes Da Cunha, C.; Vechiatto, A. Guide of technique excursion of the XIV RBMCSA. In *XIV Reunião Brasileira de Manejo e Conservação do solo e da água*; UFMT: Cuiabá, Brazil, 2016; 68p.

37. Vourlitis, G.L.; de Almeida Lobo, F.; Lawrence, S.; Holt, K.; Zappia, A.; Pinto, O.B.; de Souza Nogueira, J. Nutrient resorption in tropical savanna forests and woodlands of central Brazil. *Plant Ecol.* **2014**, *215*, 963–975. [CrossRef]

38. Prado, M.J.D. Intercâmbio Gasoso e Relações Hídricas de Duas Espécies de Combretum no Pantanal Mato-Grossense. Master's Thesis, Federal University of Mato Grosso, Campo Grande, Brazil, 2015; p. 56.

39. Santos, S.A.; da Cunha, C.N.; Tomás, W.; de Abreu, U.G.P.; Arieira, J. *Plantas Invasoras no Pantanal: Como Entender o Problema e Soluções de Manejo por Meio de Diagnóstico Participativo*; Boletim de Pesquisa e Desenvolvimento 66; Embrapa Pantanal: Corumbá, Brazil, 2006; p. 45.
40. Pott, V.J.; Pott, A. *Plantas do Pantanal Corumbá: Embrapa—Centro de Pesquisa Agropecuária do Pantanal*; Embrapa Pantanal: Corumbá, Brazil, 1994; 320p.
41. Junk, W.J.; da Cunha, C.N.; Wantzen, K.M.; Petermann, P.; Strüssmann, C.; Marques, M.I.; Adis, J. Biodiversity and its conservation in the Pantanal of Mato Grosso, Brazil. *Aquat. Sci.* **2006**, *68*, 278–309. [CrossRef]
42. Rice, A.H.; Pyle, E.H.; Saleska, S.R.; Hutyra, L.; Palace, M.; Keller, M.; de Camargo, P.B.; Portilho, K.; Marques, D.F.; Wofsy, S.C. Carbon balance and vegetation dynamics in an old-growth Amazonian forest. *Ecol. Appl.* **2004**, *14*, 55–71. [CrossRef]
43. Clark, D.B. Abolishing virginity. *J. Trop. Ecol.* **1996**, *12*, 735–739. [CrossRef]
44. Stark, S.; Leitold, V.; Wu, J.; Hunter, M.; Castilho, C.; Costa, F.; McMahon, S.; Parker, G.; Shimabukuro, M.; Lefsky, M.; et al. Amazon forest carbon dynamics predicted by profiles of canopy leaf area and light environment. *Ecol. Lett.* **2012**, *15*, 1406–1414. [CrossRef]
45. Silva, A.C.; Rêgo Mendes, K.; Santos e Silva, C.M.; Torres Rodrigues, D.; Brito Costa, G.; Thainara Corrêa da Silva, D.; Rodrigues Mutti, P.; Rodrigues Ferreira, R.; Guedes Bezerra, B. Energy Balance, CO2 Balance, and Meteorological Aspects of Desertification Hotspots in Northeast Brazil. *Water* **2021**, *13*, 2962. [CrossRef]
46. Hutyra, L.R.; Munger, J.W.; Saleska, S.R.; Gottlieb, E.; Daube, B.C.; Dunn, A.L.; Amaral, D.F.; de Camargo, P.B.; Wofsy, S.C. Seasonal controls on the exchange of carbon and water in an Amazonian rain forest. *J. Geophys. Res.* **2007**, *112*, 1–16. [CrossRef]
47. Reichstein, M.; Falge, E.; Baldocchi, D.; Papale, D.; Aubinet, M.; Berbigier, P.; Bernhofer, C.; Buchmann, N.; Giulmanov, T.; Granier, A.; et al. On the separation of net ecosystem exchange into assimilation and ecosystem respiration: Review and improved algorithm. *Glob. Change Biol.* **2005**, *11*, 1424–1439. [CrossRef]
48. Falge, E.; Baldocchi, D.; Olson, R.; Anthoni, P.; Aubinet, M.; Bernhofer, C.; Burba, G.; Ceulemans, R.; Clement, R.; Dolman, H.; et al. Gap filling strategies for defensible annual sums of net ecosystem exchange. *Agric. For. Meteorol.* **2001**, *107*, 43–69. [CrossRef]
49. Lasslop, G.; Reichstein, M.; Papale, D.; Richardson, A.D.; Arneth, A.; Barr, A.; Stoy, P.; Wohlfahrt, G. Separation of net ecosystem exchange into assimilation and respiration using a light response curve approach: Critical issues and global evaluation. *Glob. Change Biol.* **2010**, *16*, 187–208. [CrossRef]
50. Monteith, J.L. Solar Radiation and Productivity in Tropical Ecosystems. *J. Appl. Ecol.* **1972**, *9*, 747. [CrossRef]
51. Myneni, R.; Knyazikhin, Y.; Park, T. 15. MOD15A2H MODIS/Terra Leaf Area Index/FPAR 8-Day L4 Global 500 m SIN Grid V006 [Data Set]. NASA EOSDIS Land Processes DAAC. Available online: https://catalog.data.gov/dataset/modis-terraaqua-leaf-area-index-fpar-4-day-l4-global-500m-sin-grid-v006 (accessed on 26 April 2022).
52. Rienecker, M.M.; Suarez, M.J.; Gelaro, R.; Todling, R.; Bacmeister, J.; Liu, E.; Woollen, J. 15. MERRA: NASA's Modern-Era Retrospective Analysis for Research and Applications. *J. Clim.* **2011**, *24*, 3624–3648. [CrossRef]
53. Pei, Y.; Dong, J.; Zhang, Y.; Yang, J.; Zhang, Y.; Jiang, C.; Xiao, X. Performance of Four State-of-the-art GPP Products (VPM, MOD17, BESS and PML) for Grasslands in Drought Years. *Ecol. Inform.* **2020**, *56*, 101052. [CrossRef]
54. Running, S.W.; Nemani, R.R.; Heinsch, F.A.; Zhao, M.; Reeves, M.; Hashimoto, H. A Ontinuous Satellite–derived Measure of Global Terrestrial Primary Production. *Bioscience* **2004**, *54*, 547–560. [CrossRef]
55. Friedl, M.A.; Sulla-Menashe, D.; Tan, B.; Schneider, A.; Ramankutty, N.; Sibley, A.; Huang, X. MODIS Collection 5 global land cover: Algorithm refinements and characterization of new datasets. *Remote Sens. Environ.* **2010**, *114*, 168–182. [CrossRef]
56. Zhu, X.; Pei, Y.; Zheng, Z.; Dong, J.; Zhang, Y.; Wang, J.; Chen, L.; Doughty, R.; Zhang, G.; Xiao, X. Underestimates of Grassland Gross Primary Production in MODIS Standard Products. *Remote Sens.* **2018**, *10*, 1771. [CrossRef]
57. Danelichen, V.H.M.; Biudes, M.S.; Velasque, M.C.S.; Machado, N.G.; Gomes, R.S.R.; Vourlitis, G.L.; Nogueira, J.S. Estimating of gross primary production in an Amazon-Cerrado transitional forest using MODIS and Landsat imagery. *An. Acad. Bras. Cienc.* **2015**, *87*, 1545–1564. [CrossRef]
58. Wang, J.; Dong, J.; Liu, J.; Huang, M.; Li, G.; Running, S.W.; Smith, W.K.; Harris, W.; Saigusa, N.; Kondo, H.; et al. Comparison of gross primary productivity derived from GIMMS NDVI3g, GIMMS, and MODIS in southeast Asia. *Remote Sens.* **2014**, *6*, 2108–2133. [CrossRef]
59. Kuglitsch, F.G.; Reichstein, M.; Beer, C.; Carrara, A.; Ceulemans, R.; Granier, A.; Janssens, I.A.; Köstner, B.; Lindroth, A.; Loustau, D.; et al. Characterisation of ecosystem water-use efficiency of European forests from eddy-covariance measurements. *Biogeosciences Discuss.* **2008**, *5*, 4481–4519. [CrossRef]
60. Berbigier Gier, P.; Bonnefond, J.-M.; Mellmann, P. CO2 and water vapour fluxes for 2 years above Euroflux forest site. *Agric. Forest Meteorol.* **2001**, *108*, 183–197. [CrossRef]
61. Liu, X.; Chen, X.; Li, R.; Long, F.; Zhang, L.; Zhang, Q.; Li, J. Water-use efficiency of an old-growth forest in lower subtropical China. *Sci. Rep.* **2017**, *7*, 42761. [CrossRef] [PubMed]
62. Tang, X.; Li, H.; Desai, A.R.; Nagy, Z.; Luo, J.; Kolb, T.E.; Olioso, A.; Xu, X.; Yao, L.; Kutsch, W.; et al. How is water-use efficiency of terrestrial ecosystems distributed and changing on Earth? *Sci. Rep.* **2014**, *4*, 7483. [CrossRef] [PubMed]
63. Yu, G.R.; Zhang, L.M.; Sun, X.M.; Fu, Y.L.; Wen, X.F.; Wang, Q.F.; Li, S.G.; Ren, C.Y.; Song, X.I.A.; Liu, Y.F.; et al. Environmental controls over carbon exchange of three forest ecosystems in eastern China. Glob. *Change Biol.* **2008**, *14*, 2555–2571. [CrossRef]
64. Rodrigues, A.; Pita, G.; Mateus, J.; Kurz-Besson, C.; Casquilho, M.; Cerasoli, S.; Gomes, A.; Pereira, J. Eight years of continuous carbon fluxes measurements in a Portuguese eucalypt stand under two main events: Drought and felling. *Agric. Forest Meteorol.* **2011**, *151*, 493–507. [CrossRef]

65. Law, B.E.; Williams, M.; Anthoni, P.M.; Baldocchi, D.D.; Unsworth, M.H. Measuring and modelling seasonal variation of carbon dioxide and water vapour exchange of a Pinus ponderosa forest subject to soil water deficit. *Glob. Change Biol.* **2000**, *6*, 613–630. [CrossRef]

66. Krishnan, P.; Black, T.A.; Grant, N.J.; Barr, A.G.; Hogg, E.T.H.; Jassal, R.S.; Morgenstern, K. Impact of changing soil moisture distribution on net ecosystem productivity of a boreal aspen forest during and following drought. *Agric. Forest Meteorol.* **2006**, *139*, 208–223. [CrossRef]

67. Ponton, S.; Flanagan, L.B.; Alstad, K.P.; Johnson, B.G.; Morgenstern, K.A.I.; Kljun, N.; Black, T.A.; Barr, A.G. Comparison of ecosystem water-use efficiency among Douglas-fir forest, aspen forest and grassland using eddy covariance and carbon isotope techniques. *Glob. Change Biol.* **2006**, *12*, 294–310. [CrossRef]

68. Liang, S.; Li, X.; Wang, J. Estimate of vegetation production of terrestrial ecosystem. In *Advanced Remote Sensing: Terrestrial Information Extraction and Applications*; Academic Press: Oxford, UK, 2020; pp. 581–620.

69. Costa, M.H.; Biajoli, M.C.; Sanches, L.; Malhado, A.C.M.; Hutyra, L.R.; da Rocha, H.R.; Aguiar, R.G.; de Araújo, A.C. Atmospheric versus vegetation controls of Amazonian tropical rain forest evapotranspiration: Are the wet and seasonally dry rain forests any different? *J. Geophys. Res.* **2010**, *115*, 9. [CrossRef]

70. Dalmagro, H.J.; de Lobo, F.A.; Vourlitis, G.L.; Dalmolin, Â.C.; Antunes, M.Z.; Ortíz, C.E.R.; de Nogueira, J.S. Photosynthetic parameters of two invasive tree species of the Brazilian Pantanal in response to seasonal flooding. *Photosynthetica* **2013**, *51*, 281–294. [CrossRef]

71. Dalmagro, H.J.; Lathuillière, M.J.; Vourlitis, G.L.; Campos, R.C.; Pinto, O.B.; Johnson, M.S.; Ortíz, C.E.; Lobo, F.D.A.; Couto, E.G. Physiological responses to extreme hydrological events in the Pantanal wetland: Heterogeneity of a plant community containing super-dominant species. *J. Veg. Sci.* **2016**, *27*, 568–577. [CrossRef]

72. Sanches, L.; Vourlitis, G.L.; de Carvalho Alves, M.; Pinto-Júnior, O.B.; de Souza Nogueira, J. Seasonal patterns of evapotranspiration for a Vochysia divergens forest in the Brazilian Pantanal. *Wetlands* **2011**, *31*, 1215–1225. [CrossRef]

73. Vourlitis, G.L.; de Almeida Lobo, F.; Biudes, M.S.; Rodríguez Ortíz, C.E.; de Souza Nogueira, J. Spatial Variations in Soil Chemistry and Organic Matter Content across a Vochysia Divergens Invasion Front in the Brazilian Pantanal. *Soil Sci. Soc. Am. J.* **2011**, *75*, 1554–1561. [CrossRef]

74. Sjöström, M.; Ardö, J.; Arneth, A.; Boulain, N.; Cappelaere, B.; Eklundh, L.; de Grandcourt, A.; Kutsch, W.L.; Merbold, L.; Nouvellon, Y.; et al. Exploring the potential of MODIS EVI for modeling gross primary production across African ecosystems. *Remote Sens. Env.* **2011**, *115*, 1081–1089. [CrossRef]

75. Singh, N.; Patel, N.R.; Bhattacharya, B.K.; Soni, P.; Parida, B.R.; Parihar, J.S. Analyzing the dynamics and inter-linkages of carbon and water fluxes in subtropical pine (Pinus roxburghii) ecosystem. *Agric. Forest Meteorol.* **2014**, *197*, 206–218. [CrossRef]

76. Ito, A.; Inatomi, M. Water-use efficiency of the terrestrial biosphere: A model analysis focusing on interactions between the global carbon and water cycles. *J. Hydrometeorol.* **2012**, *13*, 681–694. [CrossRef]

77. Xue, B.L.; Guo, Q.H.; Otto, A.; Xiao, J.F.; Tao, S.L.; Li, L. Global patterns, trends, and drivers of water use efficiency from 2000 to 2013. *Ecosphere* **2015**, *6*, 1–18. [CrossRef]

78. Marengo, J.A.; Torres, R.R.; Alves, L.M. Drought in Northeast Brazil—past, present, and future. *Theor. Appl. Climatol.* **2017**, *129*, 1189–1200. [CrossRef]

79. Mendes, K.R.; Campos, S.; da Silva, L.L.; Mutti, P.R.; Ferreira, R.R.; Medeiros, S.S.; Perez-Marin, A.M.; Marques, T.V.; Ramos, T.M.; de Lima Vieira, M.M.; et al. Seasonal variation in net ecosystem CO2 exchange of a Brazilian seasonally dry tropical forest. *Sci. Rep.* **2020**, *10*, 9454. [CrossRef]

80. Campos, S.; Mendes, K.R.; da Silva, L.L.; Mutti, P.R.; Medeiros, S.S.; Amorim, L.B.; dos Santos, C.A.C.; Perez-Marin, A.M.; Ramos, T.M.; Marques, T.V.; et al. Closure and partitioning of the energy balance in a preserved area of Brazilian seasonally dry tropical forest. *Agric. For. Meteorol.* **2019**, *271*, 398–412. [CrossRef]

81. Marques, T.V.; Mendes, K.; Mutti, P.; Medeiros, S.; Silva, L.; Perez-Marin, A.M.; Campos, S.; Lúcio, P.S.; Lima, K.; Reis, J.; et al. Environmental and biophysical controls of evapotranspiration from Seasonally Dry Tropical Forests (Caatinga) in the Brazilian Semiarid. *Agric. For. Meteorol.* **2020**, *287*, 107957. [CrossRef]

82. Mendes, K.R.; Batista-Silva, W.; Dias-Pereira, J.; Pereira, M.P.; Souza, E.V.; Serrão, J.E.; Granja, J.A.; Pereira, E.C.; Gallacher, D.J.; Mutti, P.R.; et al. Leaf plasticity across wet and dry seasons in Croton blanchetianus (Euphorbiaceae) at a tropical dry forest. *Sci. Rep.* **2022**, *12*, 954. [CrossRef] [PubMed]